Supporting Information

Exciton, Biexciton and Hot Exciton Dynamics in $CsPbBr_3$ Colloidal Nanoplatelets

Brener R. C. Vale,[†§] Etienne Socie,[†] Andrés Burgos-Caminal,[†] Jefferson Bettini,[‡] Marco A. Schiavon,[§] and Jacques-E. Moser[†]*

[†] Photochemical Dynamics Group, Institute of Chemical Sciences & Engineering, École Polytechnique Fédérale de Lausanne, 1015 Lausanne, Switzerland

[§] Grupo de Pesquisa Química de Materiais, Departamento de Ciências Naturais, Univ. Federal de São João Del-Rei, Campus Dom Bosco, 36301-160 São João Del-Rei, Minas Gerais, Brazil

[‡] Laboratório Nacional de Nanotecnologia, Centro Nacional de Pesquisa em Energia e Materiais, Campinas, São Paulo, Brazil

1. Methods

Chemicals and Materials. All chemicals were used as received without further purification. Cesium carbonate (Cs_2CO_3, 99.9%) (Lot # MKBS7779V), lead bromide ($PbBr_2$, 99.999%) (Lot # MKCH7695), dodecane (≥ 99%) (Lot # WXBC8792V), oleylamine (OAm, 70%) (Lot # STBF4991V), and oleic acid (OA, 90%) (Lot # MKCF0988) were purchased from Sigma-Aldrich. Methyl acetate (99+%, extra dry) (1683170), 1-octadecene (90%) (Lot # AO355864), and chlorobenzene (99.5% extra dry) (Lot # 1699491) were purchased from Across Organics. n-Hexane (≥99%) (Lot # 1880693) was purchased from Fisher Chemical, and toluene (99.5%) (Lot # 16L234020) was purchased from VWR Chemicals.

Synthesis of $CsPbBr_3$ CNPls. We used a method previously described in the literature with slight modifications. First, Cs-oleate was synthesized. In this step, we reacted 2.0 mmol Cs_2CO_3 and 2.5 mmol OA in 17.5 mL of 1-octadecene in a 50 mL three-necked flask. This mixture was degassed and dried under vacuum at 120 ºC for 60 minutes. Then, we heated the system under argonium flow to 150 ºC until all Cs_2CO_3 completely reacted with OA. Since Cs-oleate precipitates out of ODE at room temperature, it must be heated to 100 ºC before use. In the synthesis of $CsPbBr_3$ CNPls, we reacted 0.2 mmol $PbBr_2$, 0.5 mL of OA and 0.5 mL of OAm in 5 mL of dodecane in a 25 mL three-necked flask. First, we degassed and dried this mixture under vacuum at room temperature for 30 minutes. Then, the mixture was heated to 150 ºC under argonium gas. Next, we removed the system from the heat source and let it cool to room temperature. Finally, we injected 0.2 mL of the Cs-oleate solution under argonium with vigorous stirring for 20 minutes. For the purification step, we added 6 mL of methyl acetate to the CNPl solution and then centrifuged it at 5000 rpm for 5 minutes. This step was just applied to remove any large particles or aggregates. Finally, we added an additional 12 mL of methyl acetate and then centrifuged the mixture at 5000 rpm for 15 minutes. We observed that the supernatant was completely transparent without fluorescence, and the precipitate contained all the CNPls. Finally, we dispersed the CNPls in 5 mL of hexane. With this procedure, we could prepare CNPls that were stable for a long period of time.

Characterization. The TEM images and diffractions were acquired using a microscope JEOL JEM 2100F equipped with a camera Orius SC200. Ultraviolet-visible absorption spectra were acquired on a Perkin Elmer Lambda 950 UV/Vis/NIR spectrometer. Steady-state fluorescence spectra were collected on a Horiba Jobin Yvon Fluorolog-3 fluorometer. For TCSPC analysis, we used a nanoLED as a pulsed source. We used a 1.00 MHz repetition rate, with a resolution of 53 ps and an instrument response function (IRF) width of 1.3 ± 0.1 ns. Detection was performed at 90º relative to the excitation source. The fluorescence and absorption spectra in the steady state were acquired by using cuvettes with an optical path of 10.00 mm. For time-resolved spectroscopy, we used cuvettes with an optical path of 1.00 mm.

Ultrafast transient absorption spectra of $CsPbBr_3$ CNPls were obtained using a fs chirped pulse amplified (CPA) Ti:sapphire laser (Clark-MXR, CPA-2001). The pump beam at 390 nm was obtained by frequency doubling the fundamental output of the laser (778 nm, 120 fs pulse duration, 1 kHz repetition rate) in a 0.5 mm-thick BBO crystal. The probe beam was produced by focusing

a portion of the fundamental of the laser into a oscillating CaF_2 crystal, yielding a white light continuum spanning from 400 to 780 nm. The probe light used in all experiments had a smaller beam cross section and a weaker intensity compared to the pump beam as to obtain a homogenous probe area. The pump beam was chopped at 500 Hz. The dynamics of the photoinduced spectra were determined using a digitally controlled delay stage (PI) in the pump path. The probe beam was split before the sample into reference and a signal branches, with the latter going through the sample, and both were separately sent into respective spectrographs (Princeton Instruments, Spectra Pro 2150i) and detected shot-to-shot by CCD cameras (Hamamatsu S07030-0906). The time resolution of the experiment was calculated to be 250 fs.[1]

FLUPS measurements were achieved using a CPA Ti:sapphire laser (Libra, Coherent) producing 45 fs pulses centered at 800 nm with a 1 kHz repetition rate. Seventy-five percent of the beam was transmitted to a white-light-seeded optical parametric amplifier (OPerA-Solo, Coherent) to generate 110 μJ gate pulses at 1300 nm. The rest of the original beam was frequency doubled to 400 nm by a type I BBO crystal to excite the sample. The sample solution was moved by a tiny argon flow to avoid bleaching. A small beam stop and a 400 nm filter were used to block most of the transmitted 400 nm pump light. The remaining FLUPS instrument (LIOP-TEC) was described earlier:[2] The horizontally polarized gate beam and vertically polarized fluorescence interacted in a 100 μm-thick BBO crystal (Eksma), which had an optical axis in the horizontal plane. The upconverted signal was generated by type II sum frequency generation since the two inputs had different polarizations. This configuration is suitable for obtaining a broad frequency range. The large angle between the fluorescence and the gate, 21° here, helps meet the phase matching requirement and background-free detection of the signal. The signal was focused onto a fiber by a concave mirror, while the frequency doubled gate beam and the upconverted pump beam were sent away. The fiber transmitted the light to a so-called unfolded Czerny-Turner spectrograph. The incoming signal was separated by wavelength through a UV grating and sent to a CCD camera (Newton 920, Andor). The dynamics of the fluorescence signal were obtained with a computer-controlled delay stage (PI) in the pump path. Anisotropy measurements were achieved by placing a λ/2 plate after the delay line. The polarization was usually set to the magic angle (54.7°) to consider only the population dynamics. The time correction and the IRF width were calculated to be 190 fs using the cross correlation between the pump and the probe. The time resolution of the experiment was 190 fs. For FLUPS measurements, we dissolved $CsPbBr_3$ CNPls into dodecane to

avoid concentration of the solution during the experiments. We performed the measurements in both dodecane and hexane. However, because of concentration of the solution due to evaporation, the emission of hot excitons was difficult to detect, which comes from the short Stokes shift of the sample. The optical density used in FLUPS at 400 nm was 0.5, and that used in TAS at 390 nm was 0.3.

2. Equation Fitting

The fitting procedure performed in this work was carried out using a multiple exponential function with a global fitting, in which all the time constants were linked to each other depending on the fluence. When necessary, the exponential function was convoluted with the IRF.

$$\Delta A\ (\lambda,t) = \mathrm{A}_1 \cdot \exp\left(\frac{-t}{\tau_1}\right) + \mathrm{A}_2 \cdot \exp\left(\frac{-t}{\tau_2}\right) \qquad \text{(S1)}$$

Table S1. Transient absorption fitting parameters from the B1 decay

$\langle N_x \rangle$	**0.26**	**0.43**	**0.86**	**1.3**	**2.1**	**2.6**	**3.5**	**4.3**
$\mathbf{A_1}$	–0.35 ± 0.03	–1.78 ± 0.03	–3.45 ± 0.03	–4.84 ± 0.03	–5.81 ± 0.03	–6.87 ± 0.03	–6.74 ± 0.03	–8.94 ± 0.03
$\boldsymbol{\tau_1}$**/ps**	10.79 ± 0.01	10.79 ± 0.01	10.79 ± 0.01	10.79 ± 0.01	10.79 ± 0.01	10.79 ± 0.01	10.79 ± 0.01	10.79 ± 0.01
$\mathbf{A_2}$	–0.68 ± 0.02	–2.46 ± 0.02	–3.39 ± 0.02	–4.56 ± 0.02	–4.97 ± 0.02	–5.30 ± 0.02	–5.08 ± 0.02	–6.06 ± 0.02
$\boldsymbol{\tau_2}$**/ps**	3366 ± 25	3366 ± 25	3366 ± 25	3366 ± 25	3366 ± 25	3366 ± 25	3366 ± 25	3366 ± 25

Table S2. FLUPS fitting parameters from the maximum decay

$< N_x >$	**0.38**	**0.80**	**1.3**	**2.5**	**3.3**	**4.3**	**6.0**
A_1	7.6 ± 0.5	17.1 ± 0.5	33.1 ± 0.5	57.6 ± 0.5	77.8 ± 0.5	93.9 ± 0.5	120.6 ± 0.5
τ_1/ps	8.3 ± 0.1	8.3 ± 0.1	8.3 ± 0.1	8.3 ± 0.1	8.3 ± 0.1	8.3 ± 0.1	8.3 ± 0.1
A_2	14.7 ± 0.3	18.6 ± 0.3	26.6 ± 0.3	37.4 ± 0.3	42.0 ± 0.3	47.4 ± 0.3	52.5 ± 0.3
τ_2/ps	2035 ± 48	2035 ± 48	2035 ± 48	2035 ± 48	2035 ± 48	2035 ± 48	2035 ± 48

3. Global Analysis

Global analysis was carried out in this work to assess the decay from hot excitons and band-edge exciton formation. We applied a triexponential model, in which all the traces were forced to evolve with the same time constants. We extracted the kinetic traces every 2 nm from 410 to 520 nm. Since we already fitted the maximum decay from 1 to 1000 ps to a biexponential function with two time constants (τ_2 = 8 ps, and τ_3 > 2000 ps), we used these values as an initial guess in our routine (fast convergence), and we fitted the data from 0.1 to 1000 ps to extract the short decay and rise components. Then, we linked all three time constants for all kinetic traces. Finally, we extracted the amplitude coefficients for each time constant (τ_1, τ_2, and τ_3) as A_1, A_2, and A_3 for each trace and plotted the amplitude *versus* wavelength.

4. Quantum Well Model

We applied the well-known model used for quantum wells to fit the absorption spectra of $CsPbBr_3$ CNPls.[3,4] Basically, this model consists of the contributions of the exciton and continuous bands.

$$A(E) = \mathrm{c}\ \alpha(E) \tag{S2}$$

A(E) is the absorbance dependent on the photon energy, c is the weight, and $\alpha(E)$ is the absorption strength of the band-edge excitons, which is given by

$$\alpha(E) = \mathrm{X}(E) + \mathrm{Con}(E) \quad \text{(S3)}$$

where X(E) and Con(E) are the exciton and continuous band absorption, respectively. X(E) and Con(E) are given by

$$\mathrm{X}(E) = \frac{1}{2\eta}\left[\mathrm{ERF}\left(\frac{E-\mathrm{E_x}}{\mathrm{w_x}} - \frac{\mathrm{w_x}}{2\eta}\right) + 1\right]\mathrm{Exp}\left(\frac{\mathrm{w_x^2}}{4\eta^2} - \frac{E-\mathrm{E_x}}{\eta}\right) \quad \text{(S4)}$$

$$\mathrm{Con}(E) = \frac{\mathrm{H}}{2}\left[\mathrm{ERF}\left(\frac{E-\mathrm{E_x}-\mathrm{E_b}}{\mathrm{w_c}}\right) + 1\right] \quad \text{(S5)}$$

where E_x , E_b , W_x , W_c , H, and η are the exciton transition energy, exciton binding energy, exciton peak width, continuum edge width, continuum edge step height, and asymmetric broadening, respectively.

Using this model, we found the values shown in Table S3.

Table S3. Parameters obtained from the fitting of the absorption spectrum using the quantum well model.

Parameters	**Values**
C	$0.0186 \pm 3\text{x}10^{-4}$ eV
E_x	$2.7516 \pm 5\text{x}10^{-4}$ eV
E_b	0.350 ± 0.010 eV
W_x	$0.0363 \pm 5\text{x}10^{-4}$ V
W_c	$0.317 \pm 5\text{x}10^{-3}$ V
H	8.8 ± 0.2 eV
η	$0.077 \pm 2\text{x}10^{-3}$ eV

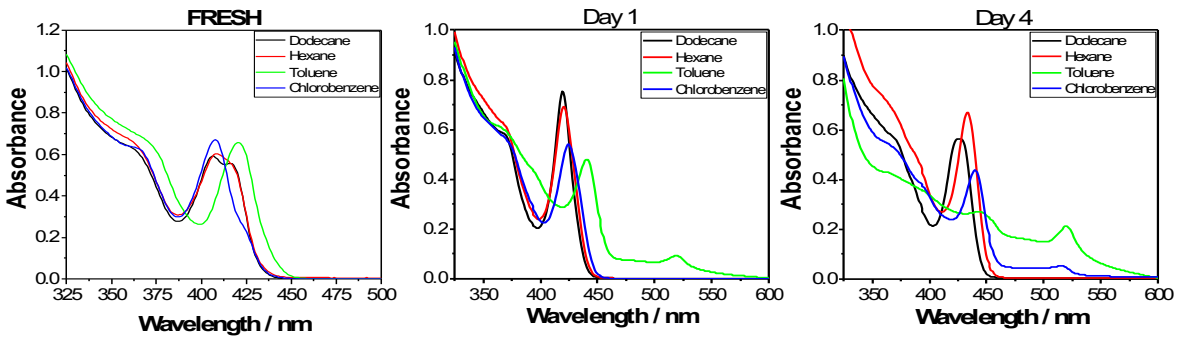

Figure S1. Stability of the prepared colloid in various solvents.

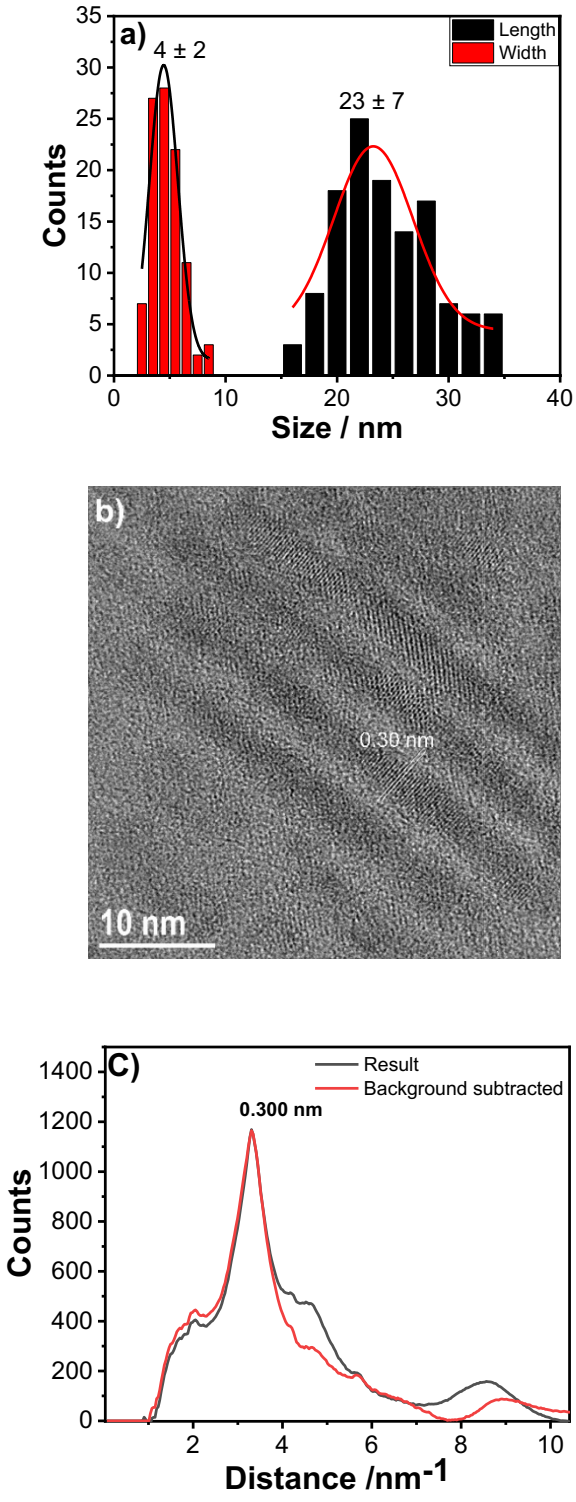

Figure S2. a) Histogram for the length and width of $CsPbBr_3$ CNPls, b) HRTEM, and c) diffraction profile obtained from TEM measurements of $CsPbBr_3$ CNPls.

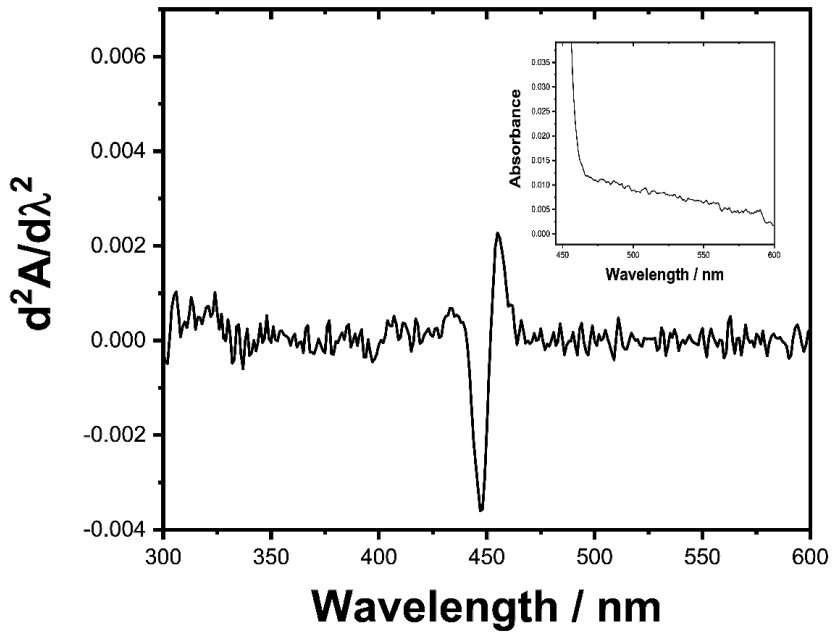

Figure S3. Second-order derivative absorption spectrum for $CsPbBr_3$ NPs.

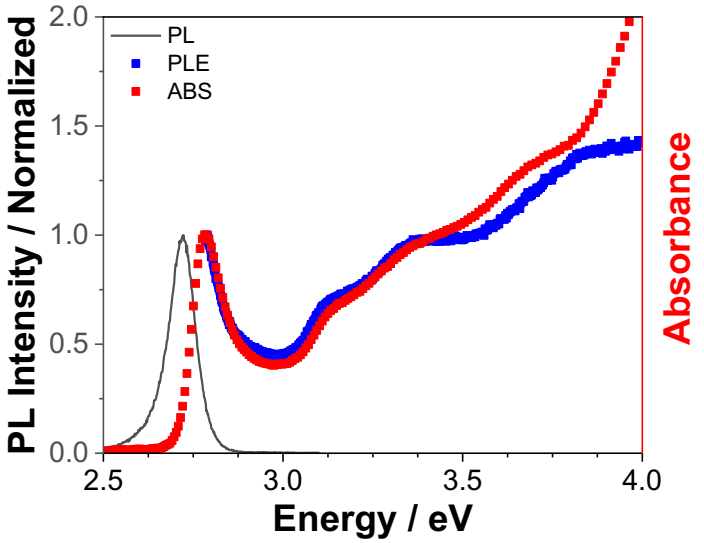

Figure S4. Emission, absorption and photoluminescence excitation spectra.

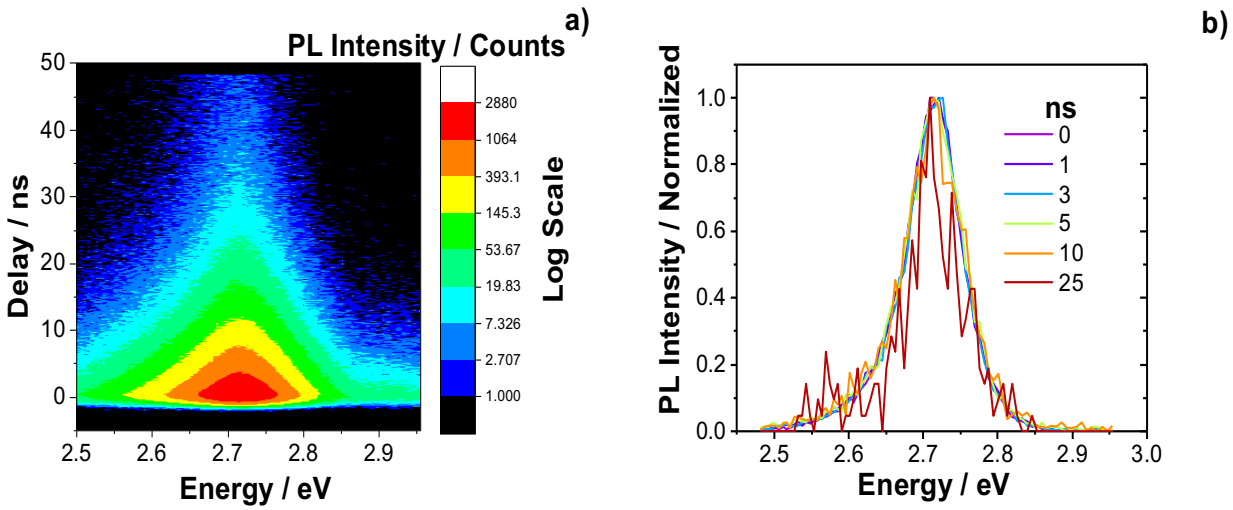

Figure S5. a) Two-dimensional of Time-Resolved Emission Spectra (TRES) in nanosecond timescale, b) Emission spectra in different time delay.

We recorded time-resolved emission spectra (TRES) in nanosecond timescale to confirm that the shoulder at lower energy in the emission spectrum does not come from different sizes or morphology. This result in nanosecond time scale, along with other ones provided by TAS and FLUPS, clearly show that the spectra do not shift to lower energy from fs (excluding hot exciton and biexciton emission) to ns. If there were particles with different shapes and sizes in the ensemble, we would expect shifts in both absorption and emission spectra into lower energy over time due to two process: energy transfer from smaller particles to the larger ones, and longer PL decay for larger particles compared to the smaller ones. Therefore, the tail in the emission spectra could be explained owing to shallow trap and surface states. The same asymmetric emission spectra have been observed for $CsPbBr_3$ QDs,[5] and for CNPLs.[6]

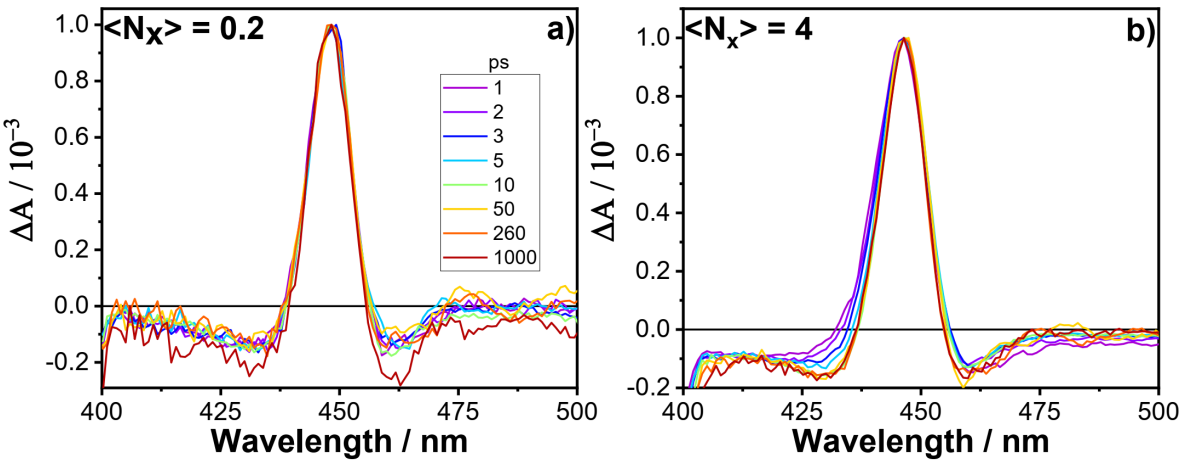

Figure S6. Normalized TA spectra of $CsPbBr_3$ NPls at a) low and b) high fluences.

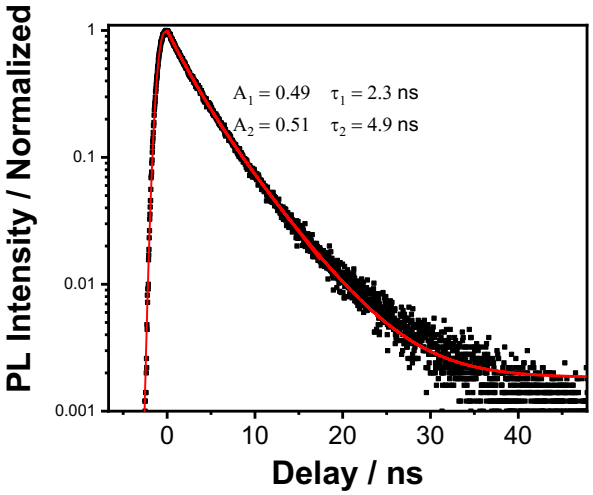

Figure S7. PL decay obtained from the TCSPC technique.

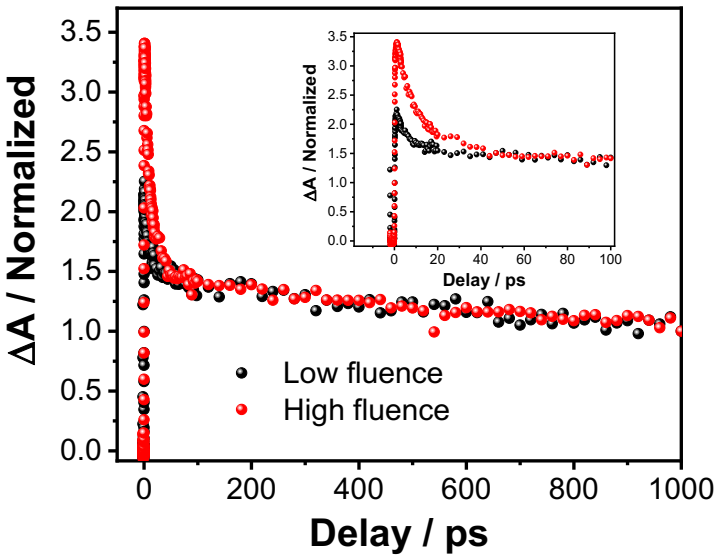

Figure S8. Bleach dynamics normalized at 1000 ps at low fluence and high fluence (inset showing the dynamics in short timescale).

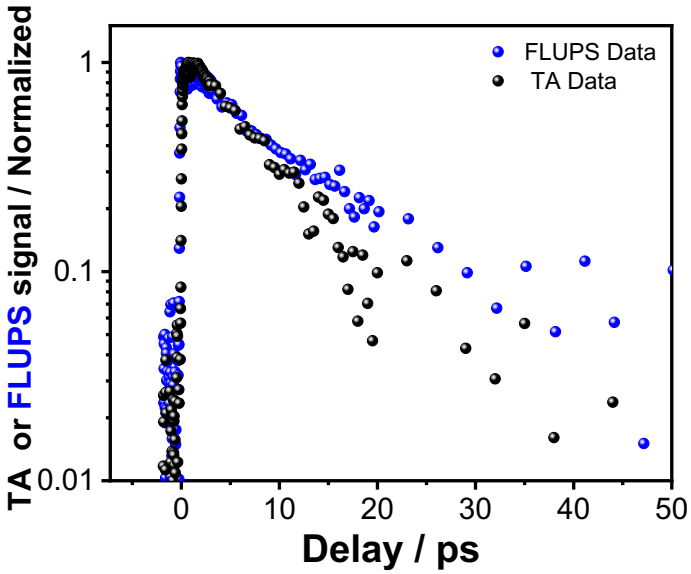

Figure S9. Biexciton Auger recombination lifetime measured by TAS and FLUPS.

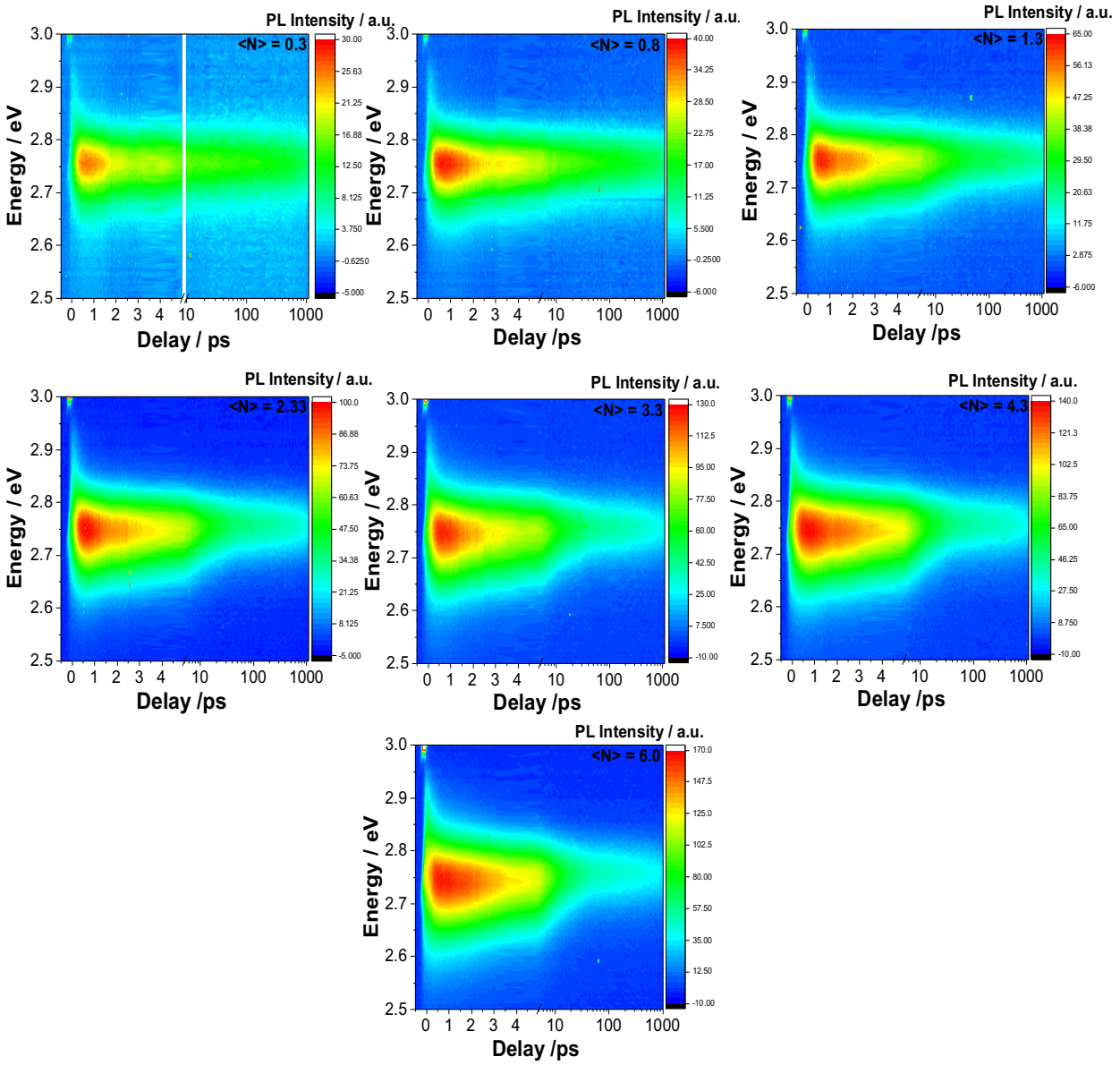

Figure S10. Two-dimensional fluorescence upconversion spectra of $CsPbBr_3$ CNPls at different pump fluences from <N> = 0.3 to 6.0.

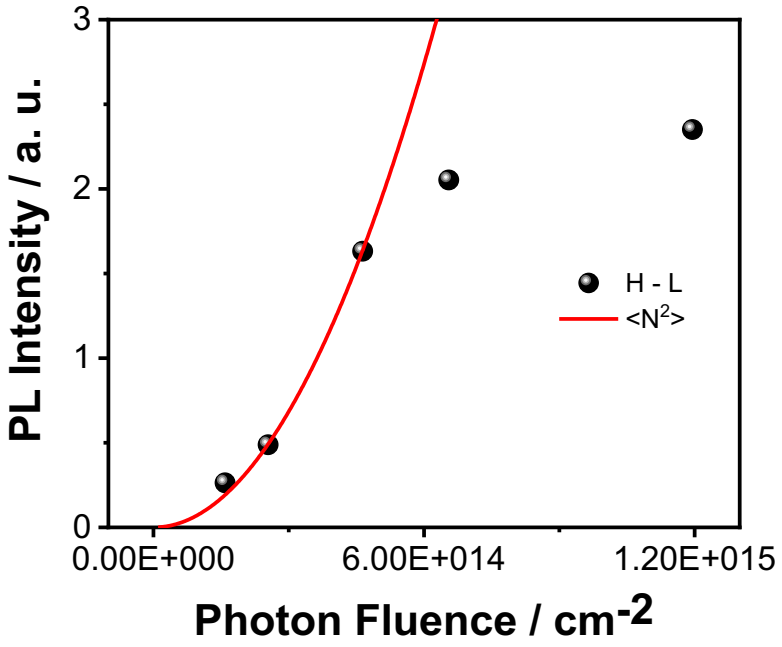

Figure S11. PL intensity was acquired by normalizing all the data at 1000 ps. H and L are higher fluence and lowest fluence. The red solid line in the figure shows the quadratic relationship. At higher fluences the system starts to saturate, and the data do not follow the quadratic behavior.

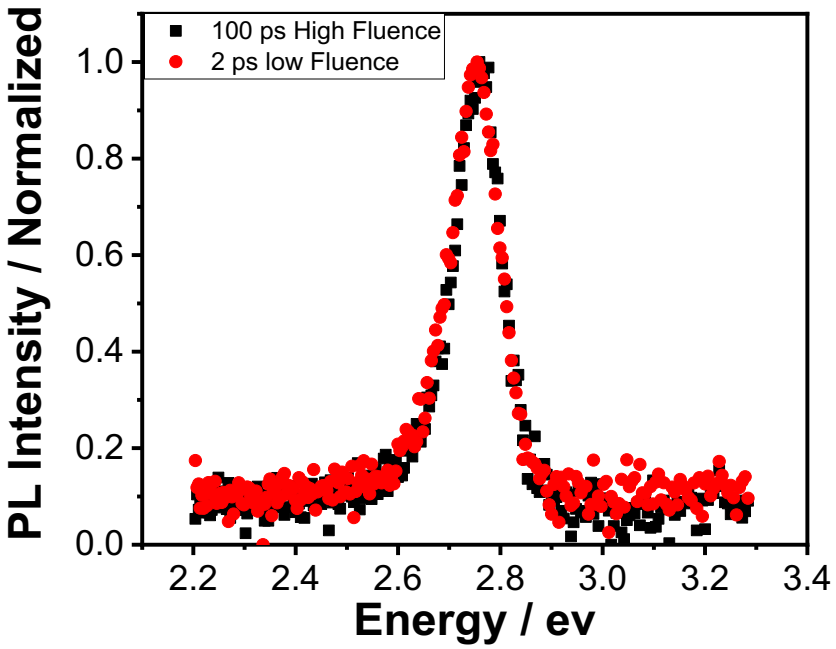

Figure S12. Fluorescence upconversion spectra at 2 ps at a low fluence and at 100 ps at a high fluence.

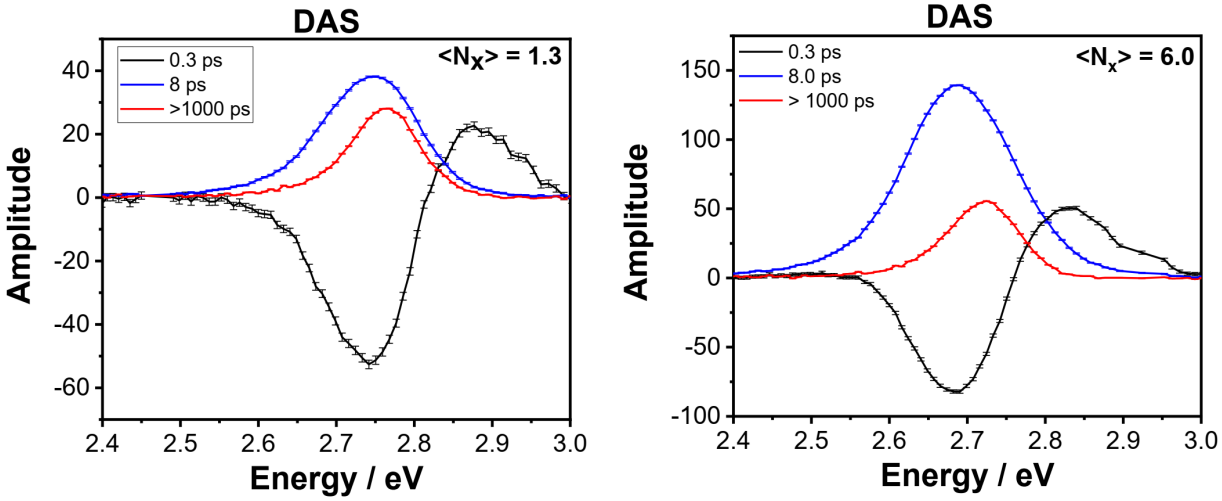

Figure S13. DAS of $CsPbBr_3$ CNPls obtained by FLUPS at different fluences of $<N_x> = 1.3$ and 6.0.

References of the Supplementary Information

(1) Bouduban, M. E. F.; Burgos-Caminal, A.; Ossola, R.; Teuscher, J.; Moser, J.-E. Energy and Charge Transfer Cascade in Methylammonium Lead Bromide Perovskite Nanoparticle Aggregates. *Chem. Sci.* **2017**, *8*, 4371–4380.

(2) Gerecke, M.; Bierhance, G.; Gutmann, M.; Ernsting, N. P.; Rosspeintner, A. Femtosecond Broadband Fluorescence Upconversion Spectroscopy: Spectral Coverage versus Efficiency. *Rev. Sci. Instr.* **2016**, *87*, 053115-1.

(3) Li, Q.; Lian, T. Ultrafast Charge Separation in Two-Dimensional $CsPbBr_3$ Perovskite Nanoplatelets. *J. Phys. Chem. Lett.* **2019**, *10*, 566–573.

(4) Li, J.; Luo, L.; Huang, H.; Ye, Z.; Zeng, J.; He, H. 2D Behaviors of Excitons in Cesium Lead Halide Perovskite Nanoplatelets. *J. Phys. Chem. Lett.* **2017**, *8*, 1161–1168.

(5) Li, J.; Gan, L.; Fang, Z.; He, H.; Ye, Z. Bright Tail States in Blue-Emitting Ultrasmall Perovskite Quantum Dots. *J. Phys. Chem. Lett.* **2017**, *8*, 6002–6008.

(6) Wu, Y.; Wei, C.; Li, X.; Li, Y.; Qiu, S.; Shen, W.; Cai, B.; Sun, Z.; Yang, D.; Deng, Z.; et al. In Situ Passivation of $PbBr_6^{4-}$ Octahedra Toward Blue Luminescent $CsPbBr_3$ Nanoplatelets with Near 100% Absolute Quantum Yield. *ACS Energy Lett.* **2018**, *3*, 2030–2037.